Empirical correlation between length of nail and system parameters for a vertical soil nailed wall

Jafar Bolouri Bazaz

Ali Akhtarpour

Ali Ahmadi

Civil Engineering Department, Ferdowsi University of Mashhad, Mashhad, Iran

akhtarpour@um.ac.ir

Abstract. The stability of excavated slopes in grounds consisting of soil or rock is one of the important topics in geotechnical engineering. The present paper deals with the global stability of a completely vertical wall excavated in non-cohesive ground reinforced by the soil nailing method. The effect of various parameters on the variation of nail length is studied based on the limit equilibrium approach by analysis of 17496 models using the SLOPE/W program. The results indicate that the length of nails increases with the reduction of internal friction angle of soil, surcharge distance from the edge of the wall, tensile strength of the nail material, and number as well as the diameter of rebars used for each nail. However, any increase in groundwater depth, the wall height, surcharge magnitude, soil unit weight, and nails spacing leads to the increased soil nail length. The novelty of current research is the derivation of empirical correlations between the system variables and the optimum length of the nail when the global factor of safety tends to a minimum required value. The relations were verified for four cases properly, which demonstrates the advantages of this study for the design of soil nailed walls.

Keywords: Soil nailing; Nail length; Wall height; Limit equilibrium method; SLOPE/W

1. Introduction

Evaluation of a soil mass condition to maintain the existing equilibrium state under applied loads is called slope stability analysis. Conventional approaches for analysis of slope stability are classified into three groups, including kinematic analysis, limit equilibrium method (LEM), and rockfall simulations. The soil nailing method was initially employed in 1960 to stabilize the wall of tunnels built in rock [1, 2]. Then, it was used widely to reinforce earthen embankments and slopes [3, 4]. Most studies on stability analysis of walls reinforced by soil nailing have been carried out based on applying the 2D finite element method (FEM). For example, Johari *et al*. [5] investigated the tensile strength and pullout strength of nailed walls excavated in clayey sand and gravel. Besides, Tang *et al*. [6] studied the stress and lateral deformation of walls owing to the pre-stressed anchor cable in combination with soil nailing. Evaluation of lateral displacement of a slope in clay reinforced by pre-stressed nails along with Berlin wall was carried out by Eidi *et al*. [7]. In general, the results of all studies show that the effect of soil nailing in reducing lateral displacement of the wall crest is more

significant than other reinforcement systems. There are also various researches based on the FEM to investigate the influence of soil properties and nailing characteristics on slope stability. For instance, the effect of constitutive models in lateral displacement of the wall [8], tensile failure of the nails [9], the influence of wall height on the factor of safety [10], the impact of installation angle and vertical spacing of the nails upon the wall protection [11] and parametric assessment of soil cohesion on the behavior of the nailed retaining structures [12] has been investigated. Numerous researchers [13-15] have also studied the soil slopes using the finite difference method (FDM). The main output of FEM and FDM analyses is the calculation of displacements and rotation of the wall under assumptions of the continuum mechanics. It is possible that the lateral displacements of the wall meet the allowable values, but the global stability may not have been provided due to the formation of the failure wedge in soil being a discontinuous medium. Therefore, the use of LEM is reported better than other methods for some cases during the analysis of stability for the slopes created in soil [16-18].

The current paper aims to evaluate the effect of soil, groundwater table, and surcharge properties on the variation of the nails length used for a vertical soil wall under static loading. The research novelty is to construct relationships for the estimation of optimal nails length, which have the best fit to a series of data points obtained from the 2D LEM analysis. This may be useful for the economical design of the soil nailing projects.

2. Methodology

The limit equilibrium method evaluates the possibility of slipping in a particular zone inside a discrete medium such as soil or a continuous substance like a rock under loading. The basis of all proposed techniques in the limit equilibrium method is the calculation of factors resistant to movement of the slipping mass, including stresses, forces, and moments in comparison with the factors causing slip [19]. Failure surface movement within slopes is considered transitionally or rotationally. The output of limit equilibrium analysis is the calculation of the global safety factor (*FS*) of slope against failure, which simply indicates the ratio of shear strength of the mass to the applied shear stress. Theoretically, if the *FS* value becomes less than one, then the slope will experience failure. During the LEM analysis, the shear strength along the probable slip surface must be determined based on a failure criterion, such as the Mohr-Coulomb equation as follows:

$$\tau_f = c + \sigma_n \tan\phi \tag{1}$$

where τ_f is the shear strength of soil (kPa), c is the cohesion of soil (kPa), σ_n is the normal stress (kPa), and ϕ is the internal friction angle of soil (deg).

Various theories have been proposed to assess slope stability using the limit equilibrium approach. The most common methods are Ordinary or Bishop, Modified Bishop, Janbu, Spencer, Corps of engineers, Lowe-Karafiath, Sarma, and Morgenstern-Price techniques [19]. Each method is based on different assumptions. The method proposed by Morgenstern-Price is found more reliable than other ones due to the comprehensive assumptions and high accuracy for the prediction of the results in practice [19, 20]. However, the *FS* value is calculated according to all methods in the present research for comparison. As a reflection of several solutions suggested for analysis of the problem, the *FS* values are different [20]. Since the exact shape and location of the failure zone is unknown before the analysis, a probable surface is assumed. Then, it is divided into finite vertical slices, and the equilibrium condition of each slice is evaluated separately. Characteristics of the slip surface can be specified by optimizing the results during multi-stage calculations [2]. At the end of the analysis, the zone with the smallest *FS* value is defined as the critical slip surface. In general, the forces acting on a slice of the failure surface can be considered as illustrated in Figure 1.

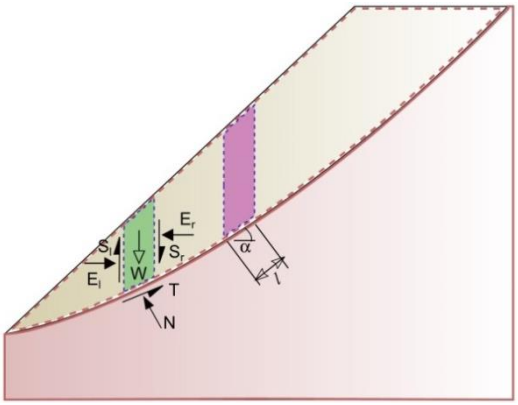

Figure 1. Schematic view of slip surface analysis with the limit equilibrium method [19]

The interaction of the left and right slices applies normal forces (E_l, E_r) and shear forces (S_l, S_r) on each side, along with the weight of each slice that produces a downward force (W). These forces are in equilibrium with force owing to the pore water pressure (N) and the reaction due to the shear stress (T). Developing the static equilibrium equations for available parameters of an unreinforced slope, the FS can be calculated from [19]:

$$FS = \frac{\sum_{i=1}^{n}\left\{\frac{[cl_i + (W_i - u_i l_i)\tan\phi]}{\cos\alpha_i + \frac{\sin\alpha_i \tan\phi}{FS}}\right\}}{\sum_{i=1}^{n}(W_i \sin\alpha_i)} \quad (2)$$

where l is the width of each slice in the failure zone (m), u is the pore water pressure (kPa), n is the total number of slices in the failure zone, and α is the base angle of each slice to the horizontal (deg).

Since the FS appears on both the right and left sides of Equation 2, an iterative calculation must be adopted to estimate it. Since the calculation process requires much time to be completed, the use of a computer program such as SLOPE/W is necessary. Besides, the formation of the failure surface was selected in the left to right direction according to the excavation position. For convergence of the results, the number of slices, FS tolerance, and minimum slip surface depth were set to 30, 0.01, and 0.1m, respectively. The local slope stability analysis necessitates the check of the lateral deformations in addition to the FS determination. However, since this research is related to the global stability of the wall, the failure zone is assumed as an integrated plate consisting of a certain number of rigid slices separate from the surrounding parts. In other words, achieving the allowable value of FS indicates slope stability. Nevertheless, the lateral deformations of the wall are controlled using PLAXIS 2D software (FEM) for some models.

3. System characteristics

The analyses are conducted for nailed walls with a height of 5, 10, and 15m excavated in cohesionless soils. The soils in this study include stiff silt, dense coarse sand, and gravel, assumed to follow the Mohr-Coulomb material model with properties summarized in Table 1.

Table 1. Characteristics of the soil (values were chosen based on [12, 21-28])

Model	γ_d (kNm^{-3})	γ_t (kNm^{-3})	γ_{sat} (kNm^{-3})	ϕ (deg)
Soil 1	12.75	14.66	17	34
Soil 2	13.60	15.64	18	36
Soil 3	14.40	16.56	19	38

In order to investigate the effect of groundwater and surcharge presence on slope stability, analyses are conducted for specific characteristics as given in Table 2.

Table 2. The surcharge and groundwater conditions (values were chosen based on [9, 18, 29])

q (kPa)	d/H	z_w/H
0, 50, 100	0, 0.2, 0.4	0, 0.33, 0.67, 1, 1.33, a*

*a presents the analysis of dry soil or a condition that groundwater level is too deep to affect the slope stability

In addition to the assumed values for z_w/H, the analyses are performed for dry soil to investigate the influence of groundwater on slope stability. From Table 2, the q=0 state is related to when the soil wall will experience no external loads, e.g., the weight of adjacent structures and forces induced by operating machines [4, 28]. The results of this condition are useful for the evaluation of the slope stability projects in non-residential areas, deserts, or coastal locations. The presence of surcharge is a conventional state for excavated walls in urban areas. Moreover, although the actual cohesion of non-cohesive soils is equal to zero based on the Mohr-Coulomb criterion, it is assumed 0.01kPa to avoid convergence difficulties during calculations. Table 3 presents the properties of the soil nailing system.

Table 3. Soil nailing parameters (values were chosen based on [9, 18, 19, 30])

f_y (MPa)	d_b (m)	L_{ini} (m)	q_b (kPa)	θ (deg)	s_v/H
380, 500, 600	0.025, 0.03	0.8H	100, 140, 180	10, 15, 20	0.1, 0.15

According to the number of states considered for variables (3×3×3×6×3×2×3×3×2) in each column of Tables 1 to 3, a total of 17496 models can be analyzed. The mechanism of slip surface formation in this research is considered based on the entry and exit method to specify the location where the trial slip surfaces probably enter the ground surface and where the surfaces will exit [27]. In other words, infinite slip surfaces within this range can be plotted and analyzed, in such a way that the slip surface with the smallest safety factor is determined as the critical slip surface. It should be noted that for a vertical wall with a height of H, the minimum required horizontal and vertical dimensions of the model may be considered as $2H$ and $4H/3$, respectively [27]. Note that L_{ini} is the initial length of nails.

In order to ensure the correctness of software performance, Rabie's work [18] was re-modeled before creating the models and starting the analysis, as shown in Figure 2. The analysis results obtained from Rabie's model indicate that the SLOPE/W program has well reproduced the critical failure surface boundary. This demonstrates the reliability of program outputs.

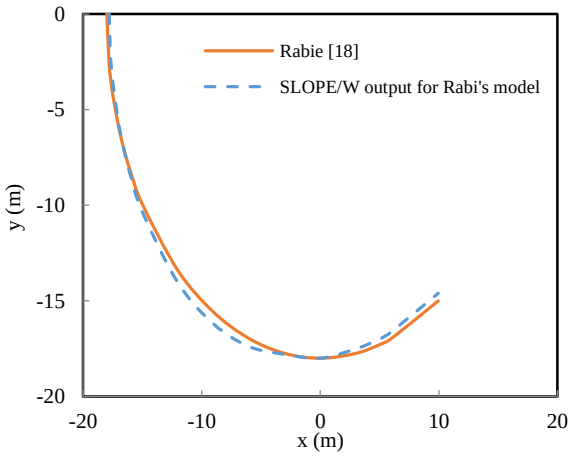

Figure 2. The robust ability of SLOPE/W to reproduce the shape of slip boundary in Rabie's model [18]

4. Results and discussion

For practical conditions, the minimum allowable value of the global safety factor to achieve the overall stability of the nailed wall in this study is assumed as FS_G=1.35 according to FHWA [30]. In each analysis, the *FS* is calculated then compared with FS_G. When $FS<FS_G$, the reinforcement system must be strengthened. Otherwise, in order to achieve an optimal design, the initial characteristics of soil nailing such as the number, type, diameter, and length of rebars used for each nail, are changed until reaching the smallest *FS* value yet bigger than FS_G. The mentioned *FS* is defined as FS_{opt} in the current research, and the length of each nail is considered the optimum soil length. Figure 3 shows the *FS* values related to the initial analysis (*FS*=1.688) and the optimal state analysis (FS_{opt}=1.357) for a given model.

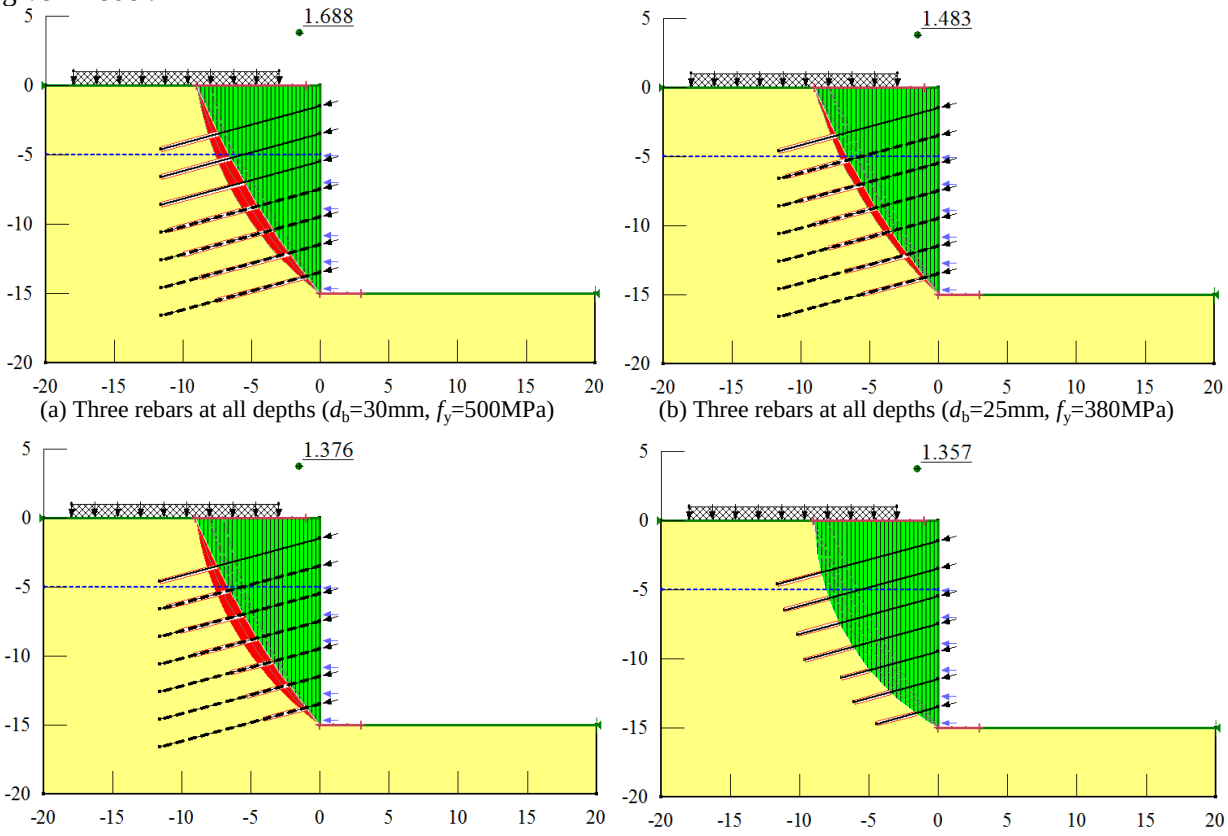

(a) Three rebars at all depths (d_b=30mm, f_y=500MPa)

(b) Three rebars at all depths (d_b=25mm, f_y=380MPa)

(c) Three rebars for nails 1-4 (d_b=25mm, f_y=380MPa) and two rebars for nails 5-7 (d_b=25mm, f_y=380MPa)

(d) Optimized state of (c) for reduced length nails

Figure 3. Analysis of a specified model with Soil 2 for H=15m, z_w=5m, θ=15°, q=50kPa, and d=3m

In Figure 3, the values shown for *FS* are calculated based on Morgenstern-Price method. However, the *FS* was also determined according to other methods for comparison. Table 4 presents the optimization process for each step of the model analysis.

Table 4. Process of optimizing the soil nailing characteristics

Analysis type	FS value (in Figure 3)			
	(a)	(b)	(c)	(d)
Morgenstern-Price	1.688	1.483	1.376	1.357
Ordinary	2.083	1.720	1.549	1.391
Bishop	1.694	1.488	1.380	1.364
Janbu	1.671	1.476	1.379	1.353
Average	1.784	1.542	1.421	1.366

Investigating all analyses demonstrates that the maximum and minimum optimum lengths, i.e., $L_{max(opt)}$ and $L_{min(opt)}$ of soil nails are required for the first and last rows of the wall, respectively. Variations of the $L_{max(opt)}/H$ against the wall height for various variables are illustrated in Figure 4.

In order to derive empirical relationships between the optimum lengths of soil nail and the problem parameters, a combined function consisting of 12 available variables (H, z_w/H, s_v/H, f_y, d_b, N_b, q_b, θ, q, d/H, γ, ϕ) was defined as:

$$\frac{L_{\min(opt)}}{H}, \frac{L_{\max(opt)}}{H} = \prod_{j=1}^{m} \left| \lambda_j x_j - \omega_j \right|^{\beta_j} \times \prod_{k=1}^{12-m} \exp\left(\lambda_k x_k\right) \tag{3}$$

where λ is the coefficient of a fitted function, x is the variable representative, ω is the constant value for a fitted function, β is the power of the fitted function, and m is the number of variables used for curve fitting by the power function.

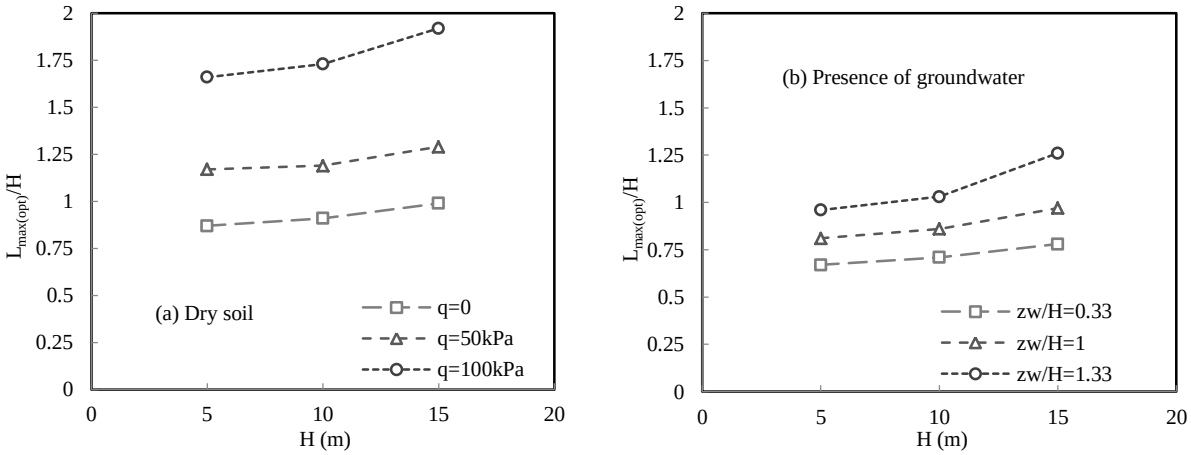

Figure 4. Variation of $L_{max(opt)}/H$ with H under different conditions for a given model

By assigning the different values for each parameter in Equation 3, the best empirical relationships are derived when the average value of correlation coefficient (R^2) for all cases reaches nearly 1. Accordingly, the R^2 values have become 0.9914 and 0.9906 for the formulas suggested to estimate the optimal values of L_{min}/H and L_{max}/H, respectively, as follows:

$$\frac{L_{\min(opt)}}{H} = 3.387 \frac{\gamma_{eq}^{0.83} s_v^{0.47}}{\phi^{0.81} N_b^{0.55} d_b^{1.86} q_b^{0.26} f_y^{0.49} H^{0.47}} \left[\frac{(30-\theta)^{0.27}}{(150-q)^{0.76}}\right] \exp\left[0.07\left(\frac{z_w}{H}\right) - 0.11\left(\frac{d}{H}\right)\right] \tag{4}$$

$$\frac{L_{\max(opt)}}{H} = 10.186 \frac{\gamma_{eq}^{0.79} s_v^{0.47}}{\phi^{0.77} N_b^{0.55} d_b^{1.86} q_b^{0.26} f_y^{0.49} H^{0.47}} \left[\frac{(30-\theta)^{0.27}}{(150-q)^{0.76}}\right] \exp\left[0.06\left(\frac{z_w}{H}\right) - 0.11\left(\frac{d}{H}\right)\right] \tag{5}$$

where s_v is the vertical spacing of nails (m), N_b is the number of rebars used for each nail, d_b is the diameter of rebars (m), q_b is the bond strength (kPa), f_y is the yield strength of rebars (MPa), H is the wall height (m), θ is the angle of nails installation from horizontal below ground surface (deg), q is the surcharge pressure (kPa), z_w is the groundwater depth (m), d is the distance of surcharge from the edge of the wall crest (m), and γ_{eq} is the equivalent unit weight of soil (kNm^{-3}) determined by:

$$\gamma_{eq} = \begin{cases} \dfrac{3\left[\gamma_d z_w + \left(\dfrac{4H}{3} - z_w\right)\left(\gamma_{sat} - \gamma_w\right)\right]}{4H}; z_w \le \dfrac{4H}{3} \\ \gamma_t \qquad\qquad ; z_w > \dfrac{4H}{3} \\ \gamma_d \qquad\qquad ; \text{Completely dry} \end{cases} \tag{6}$$

where γ_d is the dry unit weight of soil (kNm^{-3}), γ_t is the natural unit weight of soil (kNm^{-3}), γ_{sat} is the saturated unit weight of soil (kNm^{-3}), and γ_w is the unit weight of water (kNm^{-3}).

Equations 4 and 5 indicate that the length of nail increases with the reduction of internal friction angle of soil, surcharge distance from the edge of the wall, the tensile strength of the nail material, and the number and diameter of rebars used for each nail. However, any increase in groundwater depth, the height of the wall, surcharge pressure, soil unit weight, and vertical spacing of soil nails leads to the increased soil nail length. Based on the analysis outputs and empirical relations, the $L_{min(opt)}$ of soil nail is found to be about 30% to 36% of the $L_{max(opt)}$. Due to the lack of empirical or easy-to-use theoretical relationships to calculate the maximum optimal length of nails in terms of soil parameters, wall height, and surcharge characteristics, Equations 4 and 5 are innovations of the present research.

By evaluating the graphs plotted in Figure 5, it can be concluded that the minimum nail length increases with the height of the wall, in general. This can be attributed to the increase of the stress-free zone extent below the ground due to the increased excavation depth. The stress-free zone is a reflection of arching occurrence in the soil grains. In other words, the relative movement of the soil particles within the failure wedge leads to the mobilization of shear stresses and a consequent increase in the shear strength of the stagnant soil of the surrounding parts located behind the slope. Therefore, regarding the shape of the failure zone, the length of nails can be shortened at deeper rows of the wall.

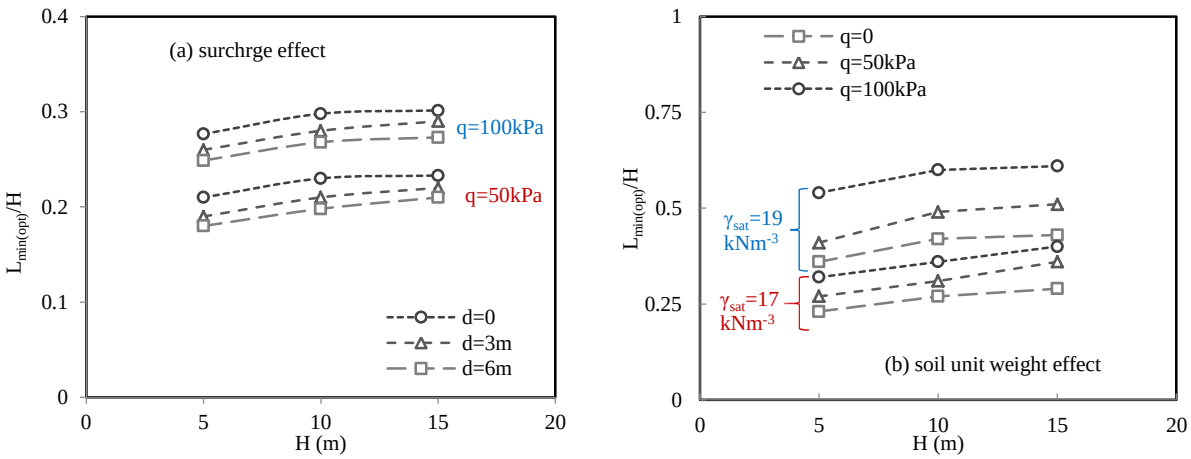

Figure 5. Influence of q, d, and γ on the variation of $L_{min(opt)}/H$ with H for specific models

The practical advantage of the empirical relations proposed in the present paper is the calculation of the nail length for the first row (Equation 4) and the last one (Equation 5). After that, considering a parabolic distribution for nail length with depth, the length (L) of other nails can be specified by:

$$L = \left\{ \frac{(H - s_{v0} - s_{vN}) L^2_{max(opt)} - (z - s_{v0}) \left[L^2_{max(opt)} - L^2_{min(opt)} \right]}{H - s_{v0} - s_{vN}} \right\}^{1/2} \quad (7)$$

where s_{v0} is the vertical distance between the top of the wall to the first row of soil nails (m), s_{vN} is the vertical distance between the deepest row of soil nails to the bottom of excavation (m), and z is the depth (m).

The validity of Equation 7 is confirmed by the data obtained from the current simulations for the time being. Hence, it needs to be checked by further studies. Finally, 100 models with the optimized nail lengths were randomly selected from 17496 models to assess lateral deformations of the walls in PLAXIS 2D software. The results of FEM analyses indicated that the maximum lateral displacements occurred at the wall crest in the range 0.00063H to 0.00092H towards the right. This demonstrates that the soil pressure on the wall has been in the active state [21]; hence, the nails were completely in

tension. Also, it can be concluded that the nailing system has given a suitable performance in stabilizing the wall.

5. Verification of empirical correlations

In order to validate the analysis results concerning the effect of the soil nailing system on the wall stability over different conditions, a comparison of several outputs with the data reported in other previous studies is definitely necessary. Table 5 summarizes the properties of four studies carried out on soil nailing.

Table 5. Available information from several studies on soil nailing

Research	Soil type	θ	s_v	f_y	d_b	N_b	q_b	ϕ	γ_{eq}	d	q	z_w	H
		(deg)	(m)	(MPa)	(m)	-	(kPa)	(deg)	(kNm^{-3})	(m)	(kPa)	(m)	(m)
Yan [9] (2D FEM)	Sandy silt	15	1.2	600	0.030	3	200	19	17	0	0	0	16
Rabie [18] (2D FEM + LEM)	Gravelly silty sand	15	0.5	400	0.025	1	120	35	19.6	0	0	0	5
Singh and Shrivastava [29] (Experimental)	Sand	15	0.1	600	0.025	1	150	31	15.05	0	1.5	0	0.3
Tatsuoka *et al.* [31] (Experimental)	Sand	10	0.1	380	0.040	1	120	31.2	15	0	1	0	0.48

The optimal values of L_{max}/H and L_{min}/H are validated by the suggested empirical correlations in Table 6. As can be seen, the small relative errors in the estimation of values for studies conducted by Yan [9], Rabie [18], Singh and Shrivastava [29], and Tatsuoka *et al.* [31] are acceptable for application in actual engineering projects. Hence, the results of this paper may be useful for the analysis and design of the various types of cohesionless soil walls reinforced by nailing system in different conditions, including the presence or absence of surcharge at the edge of the wall and the existence of groundwater, under static loading.

Table 6. Verification of empirical equations in estimating the nail length values

Research	L_{min}/H		Relative error	L_{max}/H		Relative error
	Reported	Equation 4	(%)	Reported	Equation 5	(%)
Yan [9]	0.16	0.182	+13.75	0.5	0.551	+10.20
Rabie [18]	0.50	0.512	+2.40	1.75	1.577	-9.89
Singh and Shrivastava [29]	0.60	0.623	+3.83	1.8	1.929	+7.17
Tatsuoka *et al.* [31]	0.33	0.296	-10.30	1.0	0.915	-8.50

6. Conclusion

Many slope stability analyses were performed based on the 2D limit equilibrium method to achieve a simple yet applicable manner for the optimal design of the soil nailing elements. Reinforcement of vertical walls excavated in non-cohesive soils was evaluated under different conditions. The SLOPE/W program was employed to determine the maximum and minimum optimum lengths of soil nails, when the factor of safety required for the overall stability of the wall tends to the minimum possible value of allowable *FS*. The key concluding remarks of this study can be expressed as follows:

(1) The optimum length of the nail at a given depth increases nonlinearly as a result of decreasing internal friction angle of soil and surcharge distance from the edge of the wall. Moreover, any reduction in nailing characteristics, including tensile strength of the material, installation angle as well as the number and diameter of rebars used for each nail, leads to an increase of the optimum nail length.

(2) The increased wall height, groundwater depth, surcharge pressure, soil unit weight, and vertical spacing of the nails enlarge the optimum length of the soil nail.

(3) According to the available results for four cases reported before, the empirical relationships suggested in the current paper have robust ability to reproduce the accurate value of nail length required for installation at both the first row and the deepest level of the wall.

References

[1] Baba, K., Lahcen, B., Latifa, O., Akhssas A. (2012). Slope stability evaluations by limit equilibrium and finite element methods applied to a railway in the moroccan rif. *Open Journal of Civil Engineering*, 2(1): p. 27-32.

[2] Khabbaz, H., Fatahi, B., Nucifora, C. (2012). Finite element methods against limit equilibrium approaches for slope stability analysis. In: *ANZ conference.* Melbourne, Australia: Australian Geomechanics Society, p. 1293-1298.

[3] Dey, A. (2015). Issues and aspects of soil nailing. In: *Challenges and Recent Advances in Geotechnical Engineering Research and Practice*. Guwahati, India, p. 1-21.

[4] Manjeet. (2018). A Study of Basic Elements, Types and Steps of a Soil Nailing System. *Journal of Advances and Scholarly Researches in Allied Education*, 15(3), p. 82-85.

[5] Johari, A., Hajivand, A.K., Binesh, S. (2020). System reliability analysis of soil nail wall using random finite element method. *Bull Eng Geol Environ* 79: p. 2777–2798.

[6] Tang, L., Song, M., Liao, H. (2008). Analysis of stress and deformation of prestressed anchor cable composite soil nailing. *Chinese Journal of Rock Mechanics and Engineering*, 27(9), p. 410–417.

[7] Eidi, B., Arafati, N., Mousavi, S. M., Roozmehr, F. (2013). Provide an optimum design of excavation retaining systems in clay (composite Berlin Wall and prestressed nailing system). In: *1st National Conference on Geotechnical Engineering*. Iran, Ardabil: Faculty of Engineering, Mohaghegh Ardabil University, pp. 1-8. (In Persian)

[8] Singh, V. P., Sivakumar G. L. Babu. (2010). 2D Numerical Simulations of Soil Nail Walls. *Geotechnical and Geological Engineering*, 28(4), p. 299-309.

[9] Yan, Z. G. (2012). FEM analysis of composite soil-nailing considering tensile failure. *Applied Mech Mater*, 105(07), p. 1488-1491.

[10] Ashrafi, H., Besharat, M. (2014). Investigation of sensitivity of parameters affecting the system of retaining structures by nailing method using numerical modeling. In: *8th National Congress of Civil Engineering*. Iran, Babol: Babol Noshirvani University of Technology, pp. 1-7. (In Persian)

[11] Askari, M., Mokhberi, S. M. (2017). Investigation of the effect of nail angle and distance of nails on protection of the slope using PLAXIS software. In: *4th National Conference on Recent Achievements in Civil Engineering, Architecture and Urban Planning*. Iran, Tehran: Nikan Higher Education Institute, pp. 1-14. (In Persian)

[12] Ghareh, S. (2015). Parametric assessment of soil-nailing retaining structures in cohesive and cohesionless soils. *Journal of Measurement*, 73(1), p. 341-351.

[13] Wang, J., Cao, J., Liu, H., Hu, J. (2008). Application of flac in foundation pit with compound soil nailing support. In: *4th international conference on natural computation*. Shanghai, China, p. 331-336.

[14] Rashid, A. S., Faizi, K., Kalatehjari, R., Nazir, R. (2013). Assessment of soil nailing performance by using finite element and finte difference methods. *Electronic Journal of Geotechnical Engineering*, 18(1), p. 5881-5894.

[15] Ghanbari, M., Mahani, M. S., Elahi, H. (2014). Investigation of the effect of pore water pressure and seepage force on behavior of stabilized slopes by nailing method. In: *2nd National Conference on Applied Research in Civil Engineering, Architecture and Urban Management.* Iran, Tehran: Comprehensive University of Applied Sciences, pp. 1-7. (In Persian)

[16] Villalobos E., Sergio A. V. (2020). Effect of nail spacing on the global stability of soil nailed walls using limit equilibrium and finite element methods*, Transportation Geotechnics,* p. 1-35.

[17] Cheng, Y. M., Lansivaara, T., Wei, W. B. (2007). Two-dimensional slope stability analysis by limit equilibrium and strength reduction methods. *Computers and Geotechnics*, 34(3), p. 137-150.
[18] Rabie, M. (2016). Performance of hybrid MSE/Soil Nail walls using numerical analysis and limit equilibrium approaches. *HBRC Journal*, 12(1): p. 63-70.
[19] Huang, Y. H. (2014). *Slope stability analysis by the limit equilibrium method*. American Society of Civil Engineers, p. 1-365.
[20] Tinti, S. Manucci, A. (2006). Gravitational stability computed through the limit equilibrium method revisited. *Geophysical Journal International*, 164(1), p. 1-14.
[21] Das, B. M., Sobhan, K. (2014). *Principles of Geotechnical Engineering*, Eighth Edition. Stamford, USA: Cengage Learning, p. 1-770.
[22] Zevgolis, I. E., Daffas, Z. A. (2018). System reliability assessment of soil nail walls. *Computers and Geotechnics*, 98(1), p. 232-242.
[23] Rawat, S., Gupta, A. K., Kumar, A. (2017). Pullout of soil nail with circular discs: A three-dimensional finite element analysis. *Journal of Rock Mechanics and Geotechnical Engineering*, 9(5), p. 967-980.
[24] Rawat, S., Gupta, A. K. (2017). Numerical modelling of pullout of helical soil nail. *Journal of Rock Mechanics and Geotechnical Engineering*, 9(4), p. 648-658.
[25] Yazdandoust, M. (2017). Experimental study on seismic response of soil-nailed walls with permanent facing. *Soil Dynamics and Earthquake Engineering*, 98(1), p. 101-119.
[26] Ahmadi, A., Seyedi Hosseninia, S. E. (2018). An experimental investigation on stable arch formation in cohesionless granular materials using developed trapdoor test. *Powder Technology*, 330(1), p. 137-146.
[27] GEOSLOPE Software. (2007). *GeoStudio reference manual*. [online] Calgary, Canada: GEOSLOPE International Ltd., p. 1-153. Available at: www.geoslope.com.
[28] Yazdi, J. S., Rahman, M. M., Cameron, D. A. (2014). Effect of nail layout variability on soil nailed wall analysis, In: *International Geo-Congress*. Atlanta: American society of Civil Engineers, p. 3133-3142.
[29] Singh, S., Shrivastsava, A. K. (2017). Effect of soil nailing on stability of slopes. *International Journal for Research in Applied Science & Engineering Technology*, 5(1), p. 752-763.
[30] Federal Highway Administration. (2015). *Soil nail walls reference manual*. [online] Washington, DC: U.S. Department of Transportation, p. 1-425.
[31] Tatsuoka, F., Munoz, H., Kuroda, T. (2012). Stability of existing bridges improved by structural integration and nailing. *Soils and Foundations*, 52(3), p. 430-448.